European Review for Medical and Pharmacological Sciences 2020; 24: 10632-10645

Using ultrasound three-dimensional speckle tracking technology to explore the role of SIRT1 in ventricular remodeling after myocardial infarction

Y. WANG[1], H.-F. HU[2], H.-L. LIU[1], H. LI[3], C. FENG[4], J.-J. DENG[1], L. LI[1], D.-D. ZHOU[1]

[1]Department of Ultrasound, The Second Affiliated Hospital of Qiqihar Medical College, Qiqihar, P.R. China
[2]Department of MRI, The Second Affiliated Hospital of Qiqihar Medical College, Qiqihar, P.R. China
[3]Department of Electrical Science, The Second Affiliated Hospital of Qiqihar Medical College, Qiqihar, P.R. China
[4]Department of Ultrasonography, Qiqihar Second Hospital, Qiqihar, P.R. China

Ying Wang and Haifeng Hu contributed equally to this study

Abstract. – OBJECTIVE: To investigate the role of SIRT1 in ventricular remodeling after myocardial infarction using ultrasound three-dimensional speckle tracking (3D-STI).

PATIENTS AND METHODS: Fifty-eight patients with acute myocardial infarction diagnosed in the Second Affiliated Hospital of Qiqihar Medical College from June 2015 to July 2017 were enrolled in the study. They were divided into ventricular remodeling group and ventricular non-remodeling group. Fifty-eight healthy people underwent physical examination were controls. 3D-STI was used to detect end-diastolic ventricular septal thickness (LVST), end-diastolic left ventricular posterior wall thickness (LVPWT), left ventricular end-diastolic volume (LVEDV), left ventricular end-systolic volume (LVESV), left ventricular ejection fraction (LVEF), systolic peak radial strain (PRS). SIRT1 expression levels in peripheral blood samples of the 3 groups were measured. Rats with acute myocardial infarction were treated with SIRT1 agonist. After 4 weeks, LVEDV, LVESV, LVEF, stroke volume (SV) were recorded by three-dimensional ultrasound; rat myocardial tissue protein was extracted, and SIRT1 and TGF-β, α-SMA, Vimentin and other fibrosis indicators were detected to explore the effects of SIRT1 on ventricular remodeling and myocardial fibrosis.

RESULTS: At the time of initial diagnosis, SIRT1 level in healthy group > non-ventricular remodeling group > remodeling group ($p<0.05$); at the return visit, SIRT1 levels in the remodeling group and non-ventricular remodeling group were significantly elevated ($p<0.05$), but that in the remodeling group was significantly lower than that in the non-ventricular group ($p<0.05$). The expression level of SIRT1 in H9c2 hypoxia-reperfusion cell model control group > SIRT agonist treatment model group > model group.

CONCLUSIONS: In summary, SIRT1 in the peripheral blood is negatively correlated with the degree of ventricular remodeling. The expression of SIRT1 in myocardial tissue is related to the cardiac morphology expansion and relief of reduced function in vivo after acute myocardial infarction. Up-regulation of SIRT1 expression in cell models can reduce cardiomyocyte apoptosis and inhibit cardiomyocyte fibrosis. SIRT1 has a good application prospect in predicting and treating myocardial infarction and delaying ventricular remodeling.

Key Words:
Three-dimensional speckle tracking, Myocardial infarction, Ventricular remodeling, SIRT1.

Introduction

Acute Myocardial Infarction (AMI) is a localized myocardial ischemic necrosis caused by a sudden or severe decrease in coronary blood supply. The typical clinical manifestation is sudden severe pain in the precordium region or the back of the sternum, which then radially spreads to the left shoulder, the left arm or other positions. The main cause of myocardial infarction is coronary artery atherosclerosis caused by plaque occlusion. Other causes include embolism, congenital malformation, and coronary

Corresponding Author: Ying Wang, MD; e-mail: FSEY-CSK@qmu.edu.cn

artery spasm. According to the nature of the plaque, it can be divided into stable and unstable plaques. The former has a thick fibrous cap and a small lipid core, so it is not easy to fall off; while the latter contains a large number of macrophages, and the thin fibrous cap and the large lipid core make it hard to fall off and block the coronary artery. Most patients with AMI show significant myocardial apoptosis, accompanied by elevated levels of AMI diagnostic molecular markers in peripheral blood[1]. After the onset of AMI, the loss of contractile function of the ischemic infarction causes poor coordination of ventricular wall contraction and relaxation, reduced blood emptying capacity, increased myocardial preload, changes in the morphology and function of myocardial cells and interstitial cells, disordered myocardial cells, proliferate fibroblasts, thinner ventricular septum and ventricular wall, and rounded and enlarged overall shape of the heart. Remodeling of the ventricle at the cellular and tissue levels during myocardial hypoxia-reperfusion is one of the important steps leading to pathological changes in myocardial function[2].

Three-dimensional speckle tracking imaging (3D-STI) is an innovative technique for assessing myocardial function based on speckle tracking technology and three-dimensional echocardiography[3]. The technique tracks the trajectory of myocardial motion by identifying echogenic spots on the myocardium, recording the position of the spot in each frame of the image, and comparing it with the first image to calculate the degree of deformation of the myocardium in a particular region[4]. The advantage of 3D-STI over two-dimensional speckle tracking imaging (2D-STI) is that it can track the acoustic spots on the myocardium in real time three-dimensional space, avoiding the influence of the probe angle and making up for the defects in "spot escape". Therefore, accurate and detailed depiction of the three-dimensional structural deformation of the intraventricular membrane can be performed[5].

Silent Information Regulator Factor 1 (SIRT1) belongs to the sirtuin family and is a class III histone deacetylase dependent on nicotinamide adenine dinucleotide (NAD). Expressed in prokaryotic and eukaryotes, it is involved in regulating cell metabolism, inhibiting the release of inflammatory factors, and regulating immune function[6]. SIRT1 is highly expressed in the fetal rat heart, and most of the SIRT1-deficient homozygous mice die shortly after birth due to inhibition of embryonic development during embryonic period; but there are no special changes in heart structure and function only in mice with no SIRT1 expression in the heart[7]. The latest findings suggest that SIRT1 protects the heart during the progression of cardiovascular disease[8,9]. Appropriate increase of the expression level of SIRT1 in adult rat heart can increase the tolerance of cardiomyocytes to cardiac dysfunction, apoptosis and hypertrophy[10]. Appropriate up-regulation of cardiac SIRT1 expression may attenuate ischemia-reperfusion injury, while a decrease in SIRT1 expression may exacerbate injury[11,12].

Existing studies on the use of 3D-STI for ventricular remodeling after myocardial infarction are mainly in the field of clinical case analysis; there is few research about the detection and analysis of 3D-STI index in animal models, especially rat models similar to human cardiovascular diseases. This study evaluated the 3D-STI index of cardiac structure and function in rats with acute myocardial infarction, explored the effect of SIRT1 agonist treatment on indicators, and compared trends in 3D-STI and peripheral blood SIRT1 test results in model animals and clinical cases.

Ventricular remodeling after myocardial infarction is a continuous process involving myocardial cell necrosis and disorder, fibroblast proliferation, collagen fiber deposition and tissue replacement at the molecular cell level. In view of the ability of SIRT1 to antagonize myocardial infarction and ventricular remodeling in animal, we hypothesized that SIRT1 may regulate the apoptosis of cardiomyocytes under hypoxic and reperfusion conditions at the cellular level and mimic fibrosis under the regulation of neurohumoral regulation in vivo. In this study, a hypoxic reperfusion and fibrosis cell model was established to confirm this point. The role of SIRT1 in ventricular remodeling after acute myocardial infarction was analyzed, and its mechanism at the overall level, cell level and molecular level was investigated, by studying changes in 3D-STI and serum SIRT1 levels in clinical trials after three months of initial visit and treatment, and the changes of 3D-STI results and SIRT1 protein expression in SIRT1 agonists in rats with acute myocardial infarction.

Patients and Methods

Three-Dimensional Speckle Tracking Detection

Subject information

A total of 58 patients with acute myocardial infarction in The Second Affiliated Hospital of Qiq-

ihar Medical College from June 2015 to July 2017 were enrolled, including 39 males and 19 females, 42-74 years old, with a mean age of (62.0 ± 8.4). A total of 58 healthy adults with physical examination at the same time were included as controls, including 36 males and 22 females, 28-75 years old, with a mean age of (50.5±8.1). There were no significant differences in age and gender between the two groups (p>0.05), but triglyceride (TG), total cholesterol (TCH), high-density protein cholesterol (HDL-C), low-density protein cholesterol (LDL-C) in patients with acute myocardial infarction were significantly higher than those in healthy controls ($p = 6.05\times10^{-10}$; $p = 3.62\times10^{-10}$; $p = 1.04\times10^{-9}$; $p = 1.19\times10^{-6}$; $p < 0.05$).

Inclusion and exclusion criteria

Inclusion criteria for the observation group: patients with typical acute myocardial infarction symptoms, such as persistent chest pain, chest discomfort, palpitations after exercise, chest tightness with unconsciousness, multiple changes in electrocardiogram, and changes in myocardial necrosis markers. Informed consent was obtained from all cases.

Exclusion criteria for the observation group: patients with history of old myocardial infarction, atrial fibrillation, severe valvular disease, severe liver and kidney dysfunction and unstable vital signs, artifacts due to the presence of metal foreign bodies or movements in the body; patients or their families not informed or, after informing, refused to be involved in the study.

Inclusion criteria for the control group: subjects with no abnormalities in physical examination, echocardiography, electrocardiogram, and chest X-ray examination.

Exclusion criteria for the control group: subjects with hypertension, hyperlipidemia, history of cardiovascular and cerebrovascular diseases.

Ultrasound three-dimensional speckle tracking was performed within 24 hours and 3 months after the diagnosis of acute myocardial infarction. The ultrasound three-dimensional speckle tracking technique was performed using the PHILIPS-IE33 color Doppler ultrasound imaging system produced by Philips, Eindhoven, The Netherlands. The subjects were informed of the test method and precautions before the S5-1 ultrasound probe was used. The patient was in supine position or the left lateral position according to the examination. The chest was fully exposed to connect the electrocardiogram. Firstly, the two-dimensional sonogram was used to explore the left ventricular long axis, the aortic short axis, the mitral valve broken axis, the papillary muscle short axis, the apical four-chamber and the five-chamber view. The size, shape and movement of the ventricular wall were observed, then went for the four-chamber view at the apex. After the two-dimensional image of the lesion was clearly displayed, switch to the three-dimensional mode. Full Volume mode was selected to collect the three-dimensional volume data of four consecutive cardiac cycles at the apex. Adjustments on the parameters were made to select images that met the diagnostic requirements for storage and analysis, and real-time three-dimensional QLAB post-processing software analysis was used to observe the cardiac structure using volume rendering (VR) and multiplanar recombination (MPR).

Image analysis and image post processing

Ultrasound and post-processing analysis was performed by 3 senior imaging physicians (1 chief physician and 2 deputy chief physicians). Ultrasound three-dimensional speckle tracking technique was used to calculate left ventricular end-diastolic volume (LVEDV), left ventricular end-systolic volume (LVESV), left ventricular output per volume (SV), ejection fraction (LVEF), peak time (TTP). Finally, diagnostic analysis of ultrasound three-dimensional speckle tracking data in all cases was performed to assess the probability of a patient's ventricular remodeling after acute myocardial infarction.

Peripheral blood biochemical indicators and enzyme-linked immunosorbent assay (ELISA) detection of SIRT1 protein

In the observation group and the control group, the next morning after fasting for 12 hours, 5 mL of the elbow venous blood was taken on an empty stomach. After the extraction, the blood sample was transferred to an EDTA anticoagulant tube, centrifuged at 3000 r/min for ten minutes, and the supernatant was taken. The solution was stored in a -80°C freezer. Direct detection of high-density lipoprotein cholesterol (HDL-C) and low-density lipoprotein cholesterol (LDL-C), and enzyme colorimetric detection of total cholesterol (TCH) and triacylglycerol (TG) were performed according to the manufacturer's recommended experimental methods. The content of SIRT1 in peripheral blood samples was determined by ELISA.

Rat Model of Acute Myocardial Infarction

Forty-eight Specific Pathogen Free (SPF) SD rats were numbered and randomly divided into

blank control group, model group, sham operation group and SIRT1 agonist group, with 12 rats in each group. Specific treatment: blank control group: equal amount of intraperitoneal solvent injection; model group: ligation of left anterior descending coronary artery, equal dose of intraperitoneal injection; sham operation group: suture wound after thoracotomy without ligation, equal dose of intraperitoneal injection; SIRT1 agonist group: ligation of left anterior descending coronary artery, SRT1720 20 mg/(kg · d) intraperitoneal injection. The specific method for preparing rat model of acute myocardial infarction was as follows: 30 minutes before anesthesia, morphine hydrochloride (10 mg/kg) and atropine (0.1 mg/kg) were subcutaneously injected, to respectively reduce nervous system excitability and suppress secretion; rats were anesthetized with ether and placed on a cushion with thermostat to maintain body temperature. When fully anesthetized, the rat had no righting reflex, no response to eyelid irritation, no response to pain; the muscles were relaxed, and the breathing was smooth. Then, the rat was fixed on the operating table and the chest was opened from the left 3rd to 4th intercostal space to expose the heart, and the left anterior descending coronary artery was found between the pulmonary artery cone and left atrium. The coronary artery was immediately ligated with the 0th wire, the heart was put back to the chest, and the blood and gas were squeezed out from the chest cavity. The chest cavity was immediately closed to make sure that the chest opening time did not exceed 30 s. After operation, buprenorphine (0.05 mg/kg, q12h) and meloxicam (5 mg/kg, q24h) were injected subcutaneously for analgesia, and the rats were placed on a thermal cushion in a quiet, constant temperature (27°C) in a dim room, waiting for wake-up. After waking up, the rats were placed in small cages alone to prevent fighting. New padding was used, and the troughs and drinking fountains in the cages were placed in lower places for the rats to eat and drink. To prevent postoperative infection in rats, 400,000 U of penicillin per rat was injected for 1 week. In the modeling operation, there were no deaths in the control group (n=12) and the sham operation group (n=12). In the model group (n=12), 2 died during the operation due to arrhythmia; 1 died after the operation due to heart failure. In SIRT agonist-treated group (n=12), 2 rats died during the operation due to arrhythmia. The remaining animals were euthanized by carbon dioxide inhalation 4 weeks after surgery[12]. Four weeks later, the left ventricular end-diastolic diameter, left ventricular end-systolic diameter, ejection fraction (%), and stroke volume were recorded by three-dimensional ultrasound to investigate the effect of SIRT1 agonist on new function. Euthanasia was performed after modeling. The rats were placed in a closed container for CO_2 inhalation for 10 minutes. If the rats did not move for 5 minutes, open the container. Touch the chest cavity and there was no heartbeat; touch the eyeball and there was no eyelid reflex, which means that the euthanasia was successful. Then, the heart tissue was taken and stored in liquid nitrogen. The total RNA was extracted by TRIzol method. The fibrosis indexes such as SIRT1, TGF-β, α-SMA and Vimentin were detected by fluorescence quantitative polymerase chain reaction. The effect of SIRT1 on ventricular remodeling in myocardial fibrosis was explored. This protocol has been submitted to the ethics committee and approved.

Establishment of H9c2 Cardiomyocyte Deoxygenation Reoxygenation Model

Cell culture: H9c2 rat cardiomyocytes were purchased from the cell bank of the Chinese Academy of Sciences and cultured in high glucose Dulbecco's Modified Eagle's Medium (DMEM) containing 10% fetal calf serum and 100 U/mL penicillin in an incubator with 5% CO_2 at 37°C. The medium was cultured, and the culture solution was changed every two days. The experiment was divided into control group, model group and SIRT1 agonist treatment model group. Control group: no special treatment. Model group: after the cells covered 70-80% of the medium, the medium was removed; then the medium containing 100 μmol/L of cobalt chloride was added for culture for 12 h; after replacing the medium with normal medium, the deoxygenation and reoxygenation cell model was acquired. SIRT agonist treatment model group: SRT1720 was added to the cell culture medium to a concentration of 1 μmol/L; after pretreatment for 12 hours, it was treated according to the deoxygenation /reoxygenation method of the model group.

Evaluation of cell survival using the 3-(4,5)-dimethylthiahiazo(-z-y1)-3,5-diphenytetrazoliumromide (MTT) method

H9c2 cells were first collected, and the cell suspension was inoculated into a 96-well plate at a density of 1×10^4 /well. Each group was inoculated with 12 wells, and the average of each group was taken as the final experimental result. After the inoculated cells were routinely cultured for 24

hours, they were grouped, modeled and treated according to the above treatment methods, and then the medium was discarded. 200 μL of medium with a concentration of 10% and a concentration of 5 mg/ml MTT was added to each well. The cells were cultured for 4 h in the dark; then the medium was removed, and 200 μL of dimethyl sulfoxide (DMSO) was added to each well. After shaking for 10 minutes, the absorbance at 490 nm was measured on a microplate reader. This experiment was repeated three times.

Detection of SIRT1 expression by Western blot

Each group of protein samples was extracted with total protein extraction kit. The total protein content was determined by bicinchoninic acid (BCA) method, and the protein concentration of each sample was adjusted. Then, 50 μg protein was separated by electrophoresis and transferred to polyvinylidene difluoride (PVDF) membrane. After blocking for 2 h at room temperature, SIRT primary antibody (1:1000; purchased from Abcam, Cambridge, MA, USA; item number ab110304) and β-actin primary antibody (1:2000; purchased from APPLYGEN, Beijing, China, item number C1845) were added and incubated overnight at 4°C. After rinsing with Tris-Buffered Saline and Tween-20 (TBST), secondary antibody (1:5000; purchased from Abcam, Cambridge, MA, USA; item number ab54481) was added and incubated for 2 h at room temperature. After excessive antibodies were washed away, the enhanced chemiluminescence (ECL) chromogenic kit was used to develop. After the color rendering results were scanned, the gray scale of the bands was analyzed by Image-J software, and the results were expressed as the ratio of the gray scale of the bands and the band gray scale of the internal reference β-actin.

Establishment of Angiotensin II (AngII)-Induced Rat H9c2 Cardiomyocyte Fibrosis Model

The cell lines were routinely cultured and passaged as described above. The cells were divided into control group, model group and SIRT1 inhibitor treatment model group. Control group: no special treatment. Model group: after the cells covered 70-80% of the medium, the conventional medium was removed, and the serum-free medium was added for culture for 24 hours; then, AngII was added to make the final concentration 10^{-6} μmol/L for culture for 24 hours. SIRT inhibitor treatment model group: SIRT1 inhibitor sirtnol was added to the model cell culture medium to a concentration of 40 μmol/L for treatment for 24 hours.

Expression of SIRT1 and Fibrotic Markers TGF-β, α-SMA and Vimentin in the Model Group, Control Group and SIRT Inhibitor Treatment Model Group

According to the method described above, the total protein of the control group, the model group and the SIRT1 inhibitor model group was extracted and subjected to Western blot analysis. The final result was the band gray scale ratio of the target protein and the internal reference.

Statistical Analysis

All the data obtained from the experiment were recorded in SPSS 17.0 (SPSS, Chicago, IL, USA) software for statistical analysis. The rate was compared by χ^2-test. The test level was $\alpha=0.05$, and the difference was statistically significant if $p<0.05$.

Results

Comparison of Baseline Data Between Observation Group and Control Group

There were no significant differences in age and gender between the observation group and the control group ($p<0.05$), but the differences in triacylglycerol (TG), total cholesterol (TCH), high-density lipoprotein cholesterol (HDL-C), and low-density lipoprotein cholesterol (LDL-C) were significantly different (Table I).

3D-STI Test Results

In this study, 3D-STI was performed at the first visit and three months after treatment in the observation group (including the remodeling group and the non-ventricular remodeling group), and the results of the 3D-STI test of the healthy subjects were used as controls. At the initial visit, LVEDV, LVESV, LVEF, and PRS in the non-reconstituted group ($p=0.024$; $p=0.016$; $p=0.007$; $p=0.0001$) and the reconstructed group ($p=8.93\times10^{-8}$; $p=0.0003$; $p=0.0004$; $p=1.59\times10^{-10}$) were significantly different from those in the healthy control group ($p<0.05$). At 3 months' follow-up, LVEDV, LVESV, and PRS were significantly different in the remodeling group compared with those in the initial test ($p=5.18\times10^{-7}$, $p=5.65\times10^{-10}$, $p=0.016$; $p<0.05$), while the difference of LVST, LVPWT and LVSV was not significant ($p>0.05$). The difference of LVESV in non-ventricular remodeling group was significantly different from that of the initial test ($p=1.79\times10^{-24}$; $p<0.05$).

Table I. Baseline data.

	Gender (M/F)	Age (year)	TG (mmol/L)*	TCH (mmol/L)*	HDL-C (mmol/L)*	LDL-C (mmol/L)*
Observation	39/19	62.0±8.4	1.25±0.43	3.88±0.70	1.29±0.24	2.25±0.43
Control	36/22	50.5±8.1	2.24±0.98	5.42±1.49	1.01±0.20	2.78±0.65

*The difference between the observation group and the control group was significant, $p<0.05$

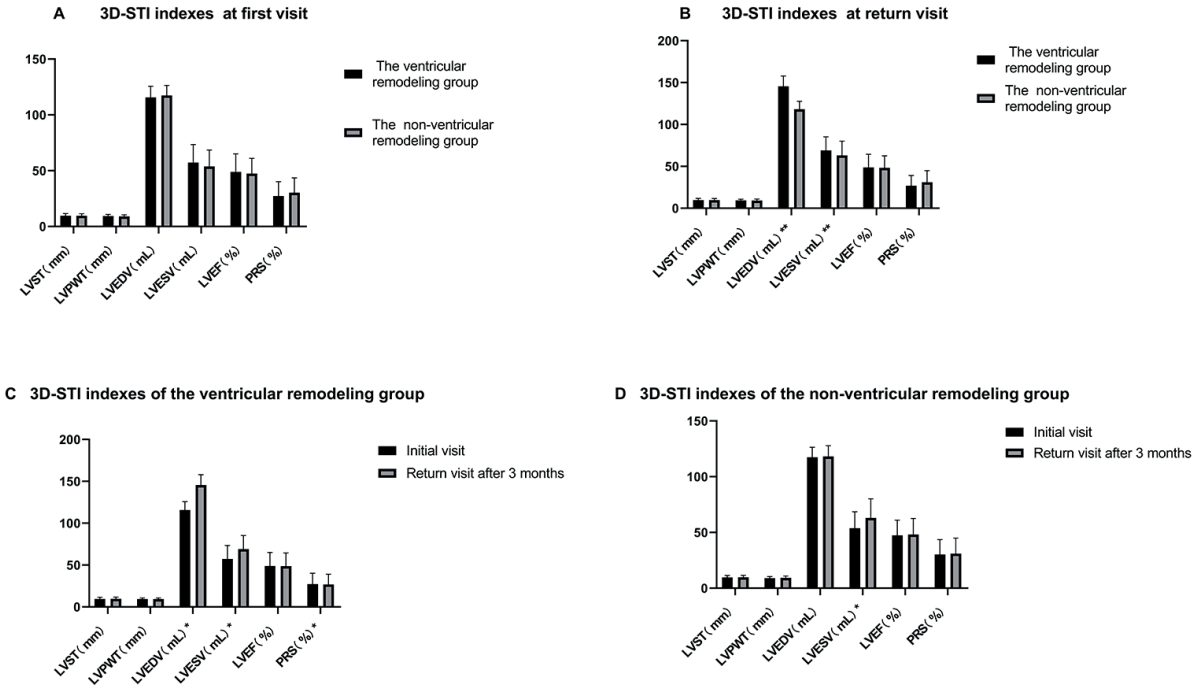

Figure 1. Changes in 3D-STI indicators in the reconstituted and non-remodeled groups at the time of initial diagnosis and after three months of treatment. **A**, 3D-STI indicators in the left ventricular remodeling group and non-ventricular group at the first visit. **B**, 3D-STI index in the left ventricular remodeling group and non-ventricular remodeling group after three months of follow-up**. C**, 3D-STI index in the left ventricular remodeling group at the time of initial diagnosis and three months return visit. **D**, 3D-STI index in the non-ventricular remodeling group at the time of initial diagnosis and three months return visit. *Significant changes between the initial diagnosis and after three months, $p<0.0$**5.** **After three months, the difference between the remodeling group and the non-ventricular remodeling group was significant, $p<0.05$

The difference of LVEDV, PRS, LVST and LVPWT was not significant. At the follow-up after 3 months, the LVESV and LVEDV were significantly different between the remodeling group and the non-ventricular remodeling group ($p=6.76\times10^{-11}$, $p=0.026$, $p<0.05$), and the difference of PRS, LVST, LVPWT was not significant ($p>0.05$) (Figure 1).

Peripheral Blood SIRT1 Protein Level Detection

At the time of initial diagnosis, the SIRT1 in the remodeling group and the non-ventricular remodeling group was significantly lower than that in the control group (12.3±1.56 ng/mL) ($p=5.72\times10^{-27}$; $p=1.74\times10^{-38}$; $p<0.05$). The difference between the remodeling and non-ventricular groups was significant ($p=4.78\times10$-77; $p<0.05$). At the return visit 3 months later, the SIRT1 in the remodeling group was significantly lower than that in the non-ventricular remodeling group ($p=0.007$; $p<0.05$), (Figure 2).

3D-STI Results of SIRT1 Agonist on Cardiac Function in Rat Model of Acute Myocardial Infarction

In all four 3D-STI parameters, there was no significant difference between the blank control

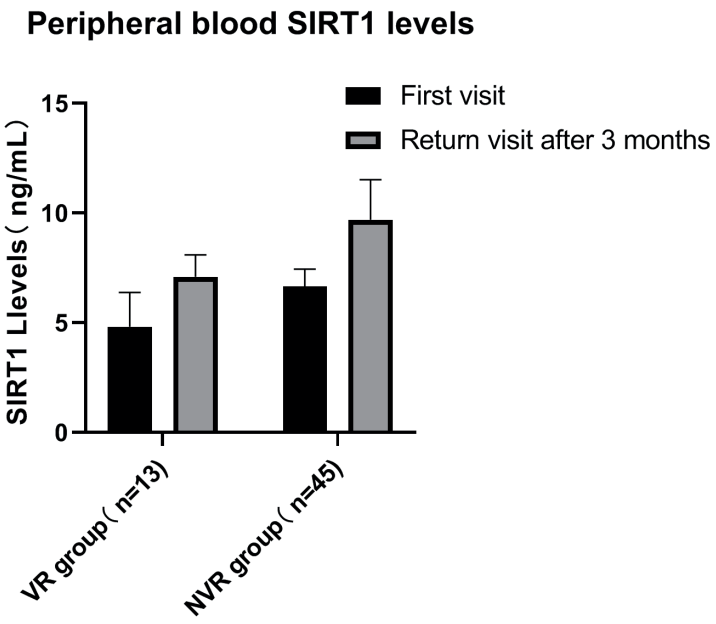

Figure 2. Peripheral blood SIRT1 levels in the remodeling and non-ventricular remodeling group at the initial diagnosis and at 3 months return visit. VR: ventricular remodeling group. NVR: non-ventricular remodeling group.

group and the sham operation group (p>0.05). The LVEDV of the model group was significantly higher than that of the blank control group (p=3.59×10^{-5}, p<0.05); LVEDV in the agonist-treated model group was significantly lower than that in the model group (p=0.03, p<0.05); LVESV in the model group was significantly higher than that in the blank control group (p=0.0007, p<0.05), the LVESV in agonist treatment model group was significantly lower than that in the model group (p=0.0004, p<0.05); the LVEF in the model group was not significantly different from that in the blank control group (p>0.05), but the LVEF in the agonist-treated model group was significantly lower than that in the model group (p=0.02, p<0.05); the SV of the model group was significantly higher than that of the blank control group (p=0.007, p<0.05), and the SV of the agonist treatment model group was significantly lower than that of the model group (p= 0.03, p<0.05) (Figure 3)

SIRT1 Agonist Treatment of Myocardial Protein Western Blot Results in a Rat Model of Acute Myocardial Infarction

In the detection of all four proteins (TGF-β, SIRT1, α-SMA, Vimentin), there was no significant difference between the blank control group and the sham operation group (p>0.05). The expression of TGF-β in the model group was significantly higher than that in the control group (p=3.29×10^{-19}, p<0.05), and significantly lower than that in the SIRT1 agonist-treated model group (p=3.85×10^{-12}, p<0.05); the expression level of SIRT1 in the model group was significantly lower than that of the control group (p= 2.07×10^{-10}, p<0.05) and SIRT1 agonist treatment model group (p=2.36×10^{-5}, p<0.05); α-SMA expression level in the model group was significantly higher than that of the control group (p=1.18×10^{-15}, p<0.05), and significantly lower than that of SIRT1 agonist treatment model group (p=1.90×10^{-12}, p<0.05); Vimentin expression in the model group was significantly higher than that in control group (p=1.70×10^{-7}, p<0.05) and significantly lower than that in the SIRT1 agonist treatment model group (p= 1.12 x 10^{-5}, p< 0.05) (Figure 4).

SIRT1 Activator Enhances Cell Viability in Deoxygenation-Reoxygenation Model

According to the results of Western blot, the SIRT expression level gray scale of the control group was 1.25±0.08, and the SIRT expression level gray scale of the deoxygenation-reoxygenation model group was 0.60±0.06, which was significantly lower than that of the control group (p<0.05). The expression level of SIRT1 in the SIRT1 activator treatment model group was 0.89±0.05, which was significantly higher than that in the model group (p<0.05).

The results of MTT assay showed that the cell viability of the control group was (0.779±0.008), and the cell viability of the deoxygenation-reoxygenation model group was (0.435±0.003), which was significantly lower than that of the control

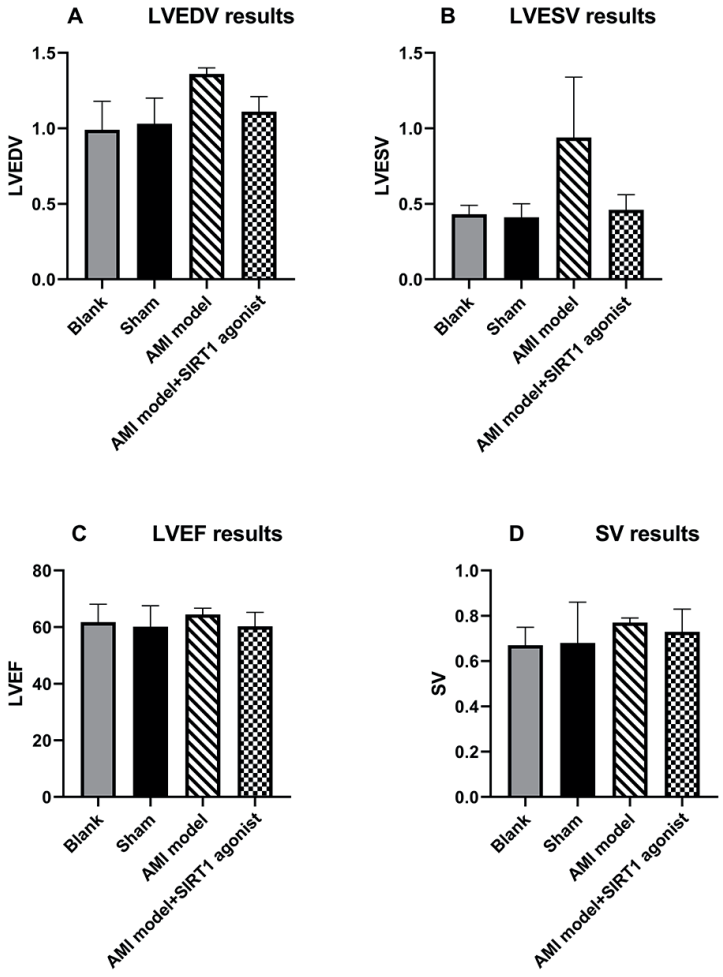

Figure 3. LVEDV, LVESV, LVEF, SV test results in the blank control group, sham operation group, model group and SIRT1 agonist treatment model group. **A**, LVEDV test results of blank control group, sham operation group, model group and SIRT1 agonist treatment model group. **B**, LVESV test results of blank control group, sham operation group, model group and SIRT1 agonist treatment model group. **C**, LVEF test results of blank control group, sham operation group, model group and SIRT1 agonist treatment model group. **D**, SV test results of blank control group, sham operation group, model group and SIRT1 agonist treatment model group.

group (p<0.05). The cell viability of the SIRT1 activator treatment model group was (0.596±0.002), which was significantly higher than that of the model group (p<0.05) (Figure 5).

Effects of SIRT Inhibitor Treatment on the Expression of SIRT1, TGF-β, α-SMA and Vimentin in the Fibrotic Model Group

According to the results of Western blot, the expression of SIRT1 in the fibrosis model group (0.55±0.02) was significantly lower than that in the control group (1.33±0.07) (p<0.05), while the TGF-β (0.56±0.05), α-SMA (1.47±0.07) and Vimentin (1.31±0.10) were significantly higher than TGF-β (0.27±0.03), α-SMA (0.61±0.02) and Vimentin (0.58±0.08) in the control group (p<0.05). In the SIRT inhibitor treatment group, SIRT1 (0.27±0.04) was significantly lower than that in the model group (p<0.05), while TGF-β (0.82±0.04), α-SMA (1.89±0.14) and Vimentin (1.65±) 0.16) were significantly higher than those in the model group (p<0.05), as shown in Figure 6.

Discussion

Silent Information Regulator Factor 1 (SIRT1) is a class III histone deacetylation that is ubiquitous in prokaryotes and eukaryotes and relies on

nicotinamide adenine dinucleotide (NAD) Enzymes; it belongs to the sirtuin protein family, has the role of regulating cell metabolism, inhibiting the release of inflammatory factors, and regulating immune function[13]. SIRT1 can inhibit the activity of inducing apoptosis by deacetylating the P53 protein, thereby enhancing the adaptability of cells to stress[14]. Daf16 is related to the longevity of C. elegans mediated by SIRT1, FOXO is a Daf16 homolog in mammals, and its family includes FOXO1, FOXO3, FOXO4 and FOXO6, which regulates the cell cycle, ROS generation, DNA repair, apoptosis[15]. SIRT1 can deacetylate and modify FOXO to activate and generate antioxidant substances such as MnSOD, etc., to improve the resistance of cells to oxidative stress[16].

This study investigated the effects of SIRT1 on ventricular remodeling after myocardial infarction and the possible mechanisms from the clinical case level, animal model level and cell model level. In clinical trials, there were no significant differences in age and gender between the observation group and the control group, but the differences were significant in triacylglycerol (TG), total cholesterol (TCH), high density lipoprotein cholesterol (HDL-C), low density lipoprotein cholesterol (LDL-C) and other indicators. At the initial visit, there was no significant difference in 3D-STI between the remodeling group and the non-ventricular remodeling group, but the remodeling group was significantly different from the observation group. After three months of treatment, the LVEDV, LVESV and PRS of the patients in the remodeling group changed significantly compared with the baseline; LVESV in non-ventricular remodeling group changed significantly, and the indicators with significant difference between remodeling group and

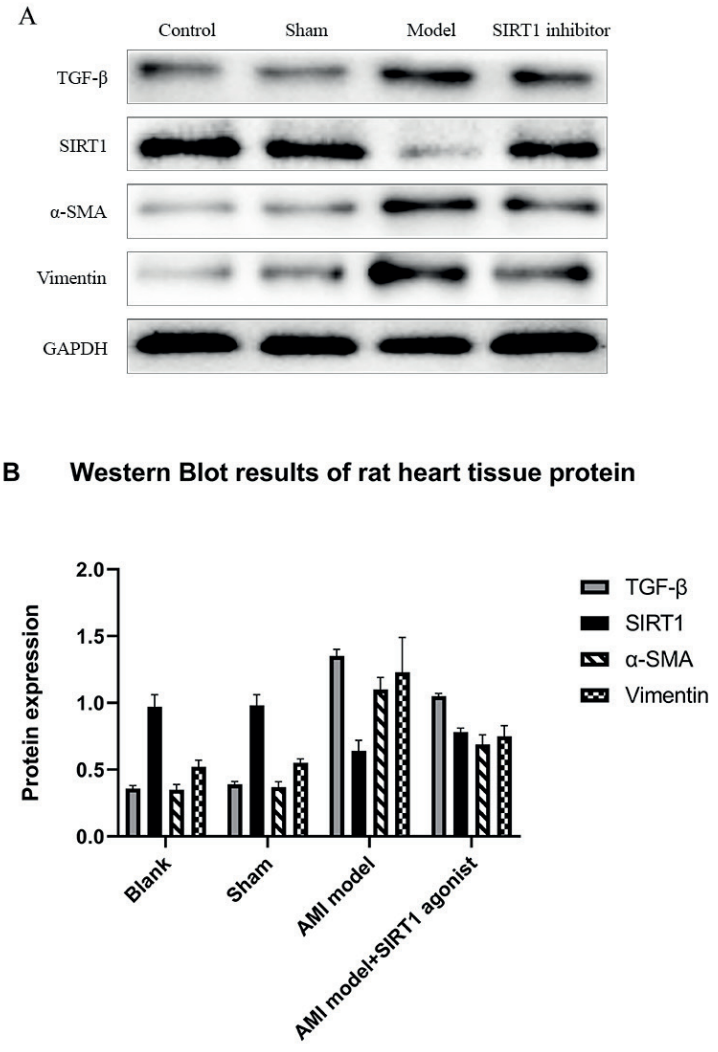

Figure 4. Expression of myocardial protein TGF-β, SIRT1, α-SMA, Vimentin in the blank control group, sham operation group, model group and SIRT1 agonist treatment group.

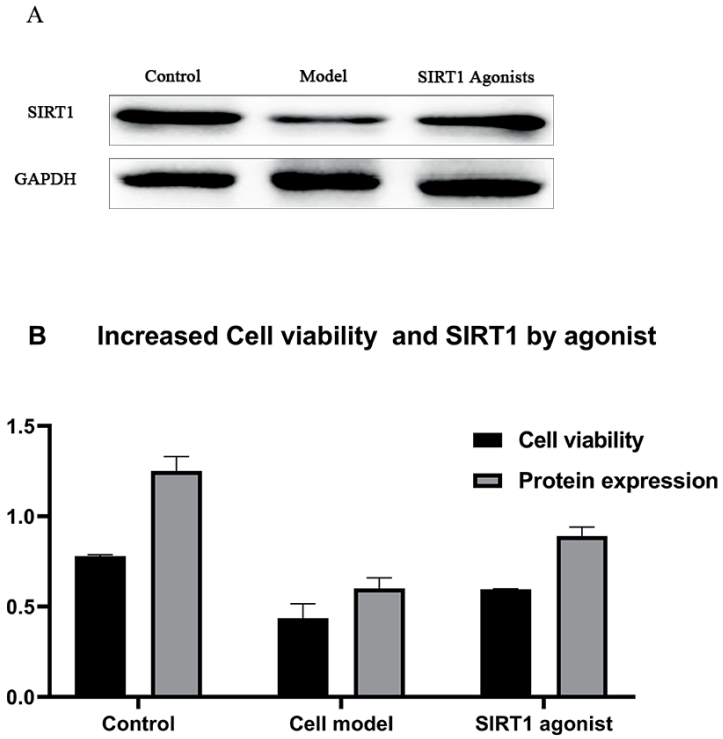

Figure 5. SIRT1 expression and cell viability after treatment with SIRT1 activator in deoxygenation-reoxygenation model cells.

non-ventricular group were LVEDV and LVESV; thus, LVEDV can be used as a predictor for left ventricular remodeling. There was no significant difference in 3D-STI between the remodeling and non-ventricular remodeling patients at baseline, but the SIRT1 level in the peripheral blood was significantly different. At the return visit, the SIRT1 levels in the peripheral blood of the remodeling and non-ventricular remodeling groups were significantly decreased compared with baseline data, and the level in remodeling group was significantly lower than that in the non-ventricular remodeling group. It can be seen that peripheral blood SIRT1 is more sensitive than LVEDV as a predictor of left ventricular remodeling, which is suitable for early prediction. The combination of SIRT1 and LVEDV can provide timely and accurate prediction of left ventricular remodeling. In the experiment of SIRT1 agonist-treated acute myocardial infarction model rats, other indicators except LVEF, namely LVEDV, LVESV, SV, were significantly different from the blank control group, while LVEDV, LVESV, LVEF, SV in the SIRT1 agonist-treated group was significantly different from those in the model group. It can be seen that SIRT1 has a significant positive effect on ventricular remodeling and its 3D-STI detection index after acute myocardial infarction; this is consistent with the protective effect of SIRT1 on myocardial protection proposed by previous studies. At the same time, the conclusions of the SIRT1 and 3D-STI detection indicators in the clinical trials of this study were also verified. In the H9c2 hypoxia-reperfusion cell model of rat cardiomyocytes, after the treatment of SIRT agonist, the expression of SIRT1 was the highest in the control group, the SIRT agonist treatment model group was the second lowest, and the model group was the lowest. The cell viability was detected by MTT assay, and cell viability was positively correlated with SIRT1 expression. Increasing the expression level of SIRT can effectively maintain cell viability and reduce apoptosis; this is consistent with the results that SIRT1 in the peripheral blood of patients in the non-ventricular remodeling group was significantly higher than that in the remodeling group. It can be seen that SIRT1 may become one of the targets for delaying ventricular remodeling and improving the prognosis of patients with myocardial infarction, which is consis-

tent with previous studies[17,18]. In the angiotensin II (AngII)-induced fibrosis model established with H9c2 cells, SIRT1 expression was the highest in the control group, followed by the model group, and the SIRT inhibitor-treated model group was the lowest. The fibrotic molecular marker α-SMA and Vimentin were the highest in the SIRT inhibitor treatment group, followed by the model group, the control group was the lowest. It can be seen that in the process of fibrosis, SIRT1 can effectively reduce the expression of inflammatory protein molecules and fibrotic molecular markers, while the decrease of SIRT1 level leads to increased levels of inflammation and fibrosis, which is also related to the results that peripheral blood SIRT1 was significantly lower in the remodeling group than that in the non-ventricular remodeling group in clinical examination. Therefore, according to the above experimental results, SIRT1 can inhibit ventricular remodeling from both aspects of reducing apoptosis and inhibiting fibrosis. Previous studies have also supported this view[19,20]. Therefore, SIRT1 has a good application prospect in predicting and treating myocardial infarction delaying ventricular remodeling.

As a newly developed echocardiographic-based diagnostic method, the principle of 3D-STI is that the ultrasonic waves emitted by the probe are reflected and scattered between the tissues in the heart, resulting in the generation of spots on the image. These spots can be displaced along with myocardial motion and its trajectory can be tracked and used to indicate myocardial activity[21]. 3D-STI has many features superior to two-dimensional echocardiography, including tracking the motion trajectory of the spot in a real-time and three-dimensional manner, and independent on the angle of incidence of the probe[22]. In view of the three-dimensional nature of cardiac function, 3D-STI can capture and describe its position and motion state more accurately in time and space, and it is clinically more advantageous. Many previous studies have confirmed this view[23-25]. In this study, 3D-STI was used to detect myocardi-

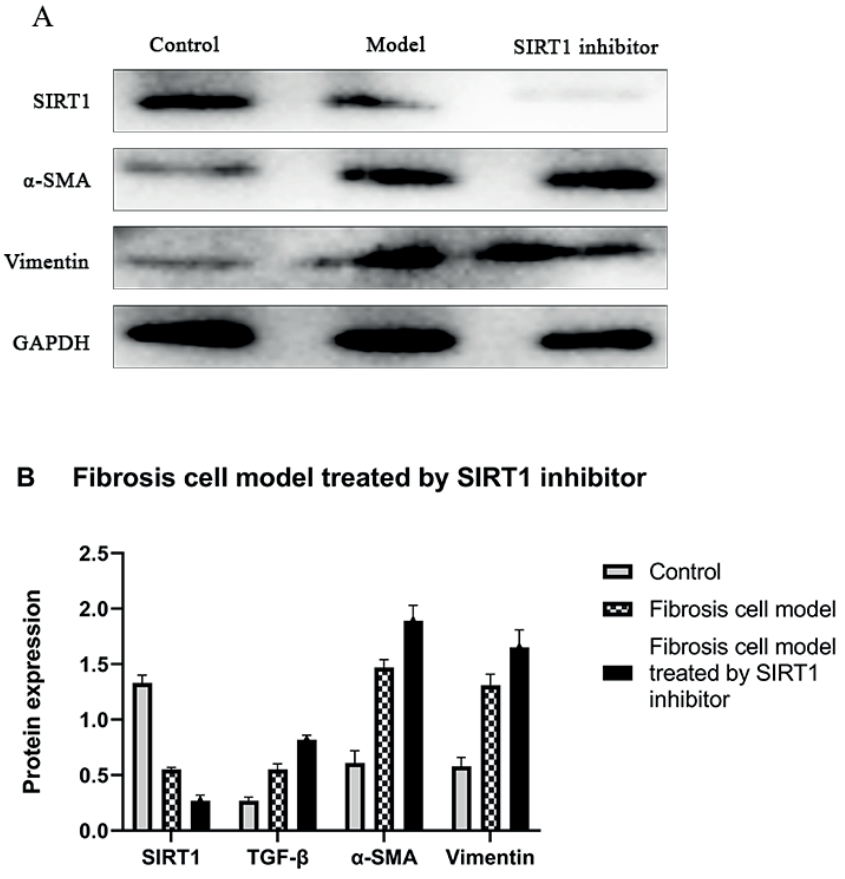

Figure 6. Expression of SIRT1, TGF-β, α-SMA and Vimentin in the fibrosis model group after SIRT inhibitor treatment.

al infarction patients, and LVEDV was selected as a predictor of left ventricular remodeling after myocardial infarction. Myocardial infarction (AMI) is an acute cause of death in cardiovascular disease. Although the rapid development of treatment in recent years has improved the short-term prognosis of AMI, the risk of long-term prognosis is still high. This is due to ventricular remodeling and eventual development into heart failure (HF) caused by AMI[26]. Ventricular remodeling occurs after AMI; myocardial hypoxia and reperfusion injury lead to myocardial necrosis and impaired exercise and function, followed by a series of pathological changes occur in the cardiomyocytes and cytoplasmic components *in vivo* under the influence of hemodynamics, inflammatory factors, immune system, and neurohumoral regulation, including cardiomyocyte hypertrophy, degeneration, necrosis, loose and disordered arrangement, increased interstitial collagen content, fibroblast activation, scar formation, thinning of myocardial tissue in the infarct site, and compensatory thickening of the myocardial tissue in the original site. The shape of the heart is blunt, ventricular function is reduced due to the overall expansion to compensate for the infarction, and the decompensation period can lead to heart failure and malignant arrhythmia[27,28]. The changes in cardiac geometry during remodeling can be described by LVST, LVPWT, and PRS, while functional changes can be described by LVEF, and LVEDV and LVESV reflect changes in morphology and function[29].

In this study, the baseline level of LVEDV was not significantly different between the remodeling group and the non-ventricular remodeling group and was significantly higher than the baseline level at the time of follow-up after three months, especially in the remodeling group. It is shown that compared with the change of left ventricular septal thickness (LVST), left ventricular posterior wall thickness (LVPWT) and peak radial strain (PRS), the ventricular dilatation develops fastest in a short time after AMI. Compared with left ventricular ejection fraction (LVEF) and left ventricular end-systolic volume (LVESV) in the compensatory period shortly after AMI, left ventricular end-diastolic volume (LVEDV) is most significantly changed due to the elongated deformation of myocardial fibers and ventricular dilatation. Therefore, LVEDV is suitable as an indicator for predicting ventricular remodeling. In the process of myocardial hypoxia-reperfusion injury and fibrosis, SIRT1 plays a role in inhibiting injury, apoptosis and fibrosis[30]. SIRT1 is a deacetylase widely distributed in mammalian cell membranes, cytoplasm and nucleus, and plays an important role in physiological and pathological processes such as energy metabolism, aging, tumor, inflammation, deoxygenation reoxygenation[31-36]. In this study, it was found that SIRT1 levels in peripheral blood of patients with myocardial infarction were inversely correlated with the degree of ventricular remodeling, whereas in the deoxygenation-reoxygenation model of cardiomyocytes, high expression of SIRT1 increased cell viability. In the cell fibrosis model, inhibition of SIRT1 expression leads to increased levels of inflammatory molecules and fibrotic markers and increased fibrosis; this is consistent with experimental results in the clinical trials in which the remodeling group has a lower SIRT1 expression than the non-ventricular remodeling group, and also consistent with the conclusions in previous studies[37,38]. Some studies have found that *in vivo* experiments, lower SIRT expression can exacerbate ventricular remodeling and myocardial damage and fibrosis[39-41], while using drugs to increase SIRT1 levels can reduce deoxygenation-reoxygenation injury[42,43], inhibit apoptosis[44], promote autophagy and delays remodeling[45,46], thereby protecting the heart[47,48].

Conclusions

In summary, this study found that 3D-STI can effectively detect changes in cardiac structure and function in patients with myocardial infarction, and the indicators of LVEDV and peripheral blood SIRT1 content are suitable for early prediction and screening of ventricular remodeling. The novelties of this study are that the results of 3D-STI clinical trials and animal experiments confirm each other, suggesting that among all the indicators (LVST, LVPWT, LVEDV, LVESV, LVEF, PRS, SV), LVEDV is the most suitable indicator for predicting ventricular remodeling. At the cellular level, animal model level and clinical level, it was confirmed that during myocardial infarction and ventricular remodeling, SIRT1 inhibited myocardial cell apoptosis and fibrosis, reduced inflammation, and delayed the process of ventricular remodeling. It is proposed that SIRT1 may become a potential therapeutic target for improving the prognosis of patients with myocardial infarction.

Conflict of Interest

The Authors declare that they have no conflict of interests.

References

1) Schaaf M, Andre P, Altman M, Maucort-Boulch D, Placide J, Chevalier P, Bergerot C, Thibault H. Left atrial remodelling assessed by 2D and 3D echocardiography identifies paroxysmal atrial fibrillation. Eur Heart J Cardiovasc Imaging 2017; 18: 46-53.
2) Barberato SH, Romano MMD, Beck ALS, Rodrigues ACT, Almeida ALC, Assunção BMBL, Gripp EA, Guimarães Filho FV, Abensur H, Castillo JMD, Miglioranza MH, Vieira MLC, Barros MVL, Nunes MDCP, Otto MEB, Hortegal RA, Barretto RBM, Campos TH, Siqueira VN, Morhy SS. Position statement on indications of echocardiography in adults – 2019. Arq Bras Cardiol 2019; 113: 135-181.
3) Hung J, Lang R, Flachskampf F, Shernan SK, McCulloch ML, Adams DB, Thomas J, Vannan M, Ryan T, ASE. 3D echocardiography: a review of the current status and future directions. J Am Soc Echocardiogr 2007; 20: 213-233.
4) Monaghan MJ. Role of real time 3D echocardiography in evaluating the left ventricle. Heart 2006; 92: 131-136.
5) Havasi K, Ambrus N, Kalapos A, Forster T, Nemes A. The role of echocardiography in the management of adult patients with congenital heart disease following operative treatment. Cardiovasc Diagn Ther 2018; 8: 771-779.
6) Doulamis IP, Tzani AI, Konstantopoulos PS, Samanidis G, Georgiopoulos G, Toutouzas KP, Perrea DN, Perreas KG. A sirtuin 1/MMP2 prognostic index for myocardial infarction in patients with advanced coronary artery disease. Int J Cardiol 2017; 230: 447-453.
7) Pillai VB, Sundaresan NR, Gupta MP. Regulation of Akt signaling by sirtuins: its implication in cardiac hypertrophy and aging. Circ Res 2014; 114: 368-378.
8) Xiao J, Sheng X, Zhang X, Guo M, Ji X. Curcumin protects against myocardial infarction-induced cardiac fibrosis via SIRT1 activation in vivo and in vitro. Drug Des Devel Ther 2016; 10: 1267-1277.
9) Li Y, Wang S, Liu B, Tang L, Kuang RR, Wang XB, Zhao C, Song XD, Cao XM, Wu X, Yang PZ, Wang LZ, Chen AH. Sulforaphane prevents rat cardiomyocytes from hypoxia/reoxygenation injury in vitro via activating SIRT1 and subsequently inhibiting ER stress. Acta Pharmacol Sin 2016; 37: 344-353.
10) Hsu CP, Zhai P, Yamamoto T, Maejima Y, Matsushima S, Hariharan N, Shao D, Takagi H, Oka S, Sadoshima J. Silent information regulator 1 protects the heart from ischemia/reperfusion. Circulation 2010; 122: 2170-2182.
11) Shalwala M, Zhu SG, Das A, Salloum FN, Xi L, Kukreja RC. Sirtuin 1 (SIRT1) activation mediates sildenafil induced delayed cardioprotection against ischemia-reperfusion injury in mice. PLoS One 2014; 9: e86977.
12) Hochman JS, Bulkley BH. Expansion of acute myocardial infarction: an experimental study. Circulation 1982; 65: 1446-1450.
13) Vaziri H, Dessain SK, Ng Eaton E, Imai SI, Frye RA, Pandita TK, Guarente L, Weinberg RA. hSIR2(SIRT1) functions as an NAD-dependent p53 deacetylase. Cell 2001; 107: 149-159.
14) Chen WY, Wang DH, Yen RC, Luo J, Gu W, Baylin SB. Tumor suppressor HIC1 directly regulates SIRT1 to modulate p53-dependent DNA-damage responses. Cell 2005; 123: 437-448.
15) Giannakou ME, Partridge L. The interaction between FOXO and SIRT1: tipping the balance towards survival. Trends Cell Biol 2004; 14: 408-412.
16) Brunet A, Sweeney LB, Sturgill JF, Chua KF, Greer PL, Lin Y, Tran H, Ross SE, Mostoslavsky R, Cohen HY, Hu LS, Cheng HL, Jedrychowski MP, Gygi SP, Sinclair DA, Alt FW, Greenberg ME. Stress-dependent regulation of FOXO transcription factors by the SIRT1 deacetylase. Science 2004; 303: 2011-2015.
17) Gao D, Zuo Z, Tian J, Ali Q, Lin Y, Lei H, Sun Z. Activation of SIRT1 attenuates Klotho deficiency-induced arterial stiffness and hypertension by enhancing AMPKα activity. Hypertension 2016; 68: 1191-1199.
18) Jian B, Yang S, Chaudry IH, Raju R. Resveratrol improves cardiac contractility following trauma-hemorrhage by modulating Sirt1. Mol Med 2012; 18: 209-214.
19) Li N, Zhou H, Ma ZG, Zhu JX, Liu C, Song P, Kong CY, Wu HM, Deng W, Tang QZ. Geniposide alleviates isoproterenol-induced cardiac fibrosis partially via SIRT1 activation in vivo and in vitro. Front Pharmacol 2018; 9: 854.
20) Wang Q, Sui X, Sui DJ, Yang P. Flavonoid extract from propolis inhibits cardiac fibrosis triggered by myocardial infarction through upregulation of SIRT1. Evid Based Complement Alternat Med 2018; 2018: 4957573.
21) Prastaro M, Pirozzi E, Gaibazzi N, Paolillo S, Santoro C, Savarese G, Losi MA, Esposito G, Perrone Filardi P, Trimarco B, Galderisi M. Expert review on the prognostic role of echocardiography after acute myocardial infarction. J Am Soc Echocardiogr 2017; 30: 431-443.e2.
22) Maffessanti F, Nesser HJ, Weinert L, Steringer-Mascherbauer R, Niel J, Gorissen W, Sugeng L, Lang RM, Mor-Avi V. Quantitative evaluation of regional left ventricular function using three-dimensional speckle tracking echocardiography in patients with and without heart disease. Am J Cardiol 2009; 104: 1755-1762.
23) Ola RK, Meena CB, Ramakrishnan S, Agarwal A, Bhargava S. Detection of left ventricular remodeling in acute ST elevation myocardial infarction after primary percutaneous coronary intervention by two dimensional and three dimensional echocardiography. J Cardiovasc Echogr 2018; 28: 39-44.
24) Mele D, Nardozza M, Chiodi E. Early speckle-tracking echocardiography predicts left ventricle re-

modeling after acute ST-segment elevation myocardial infarction. J Cardiovasc Echogr 2017; 27: 93-98.
25) Tao ZW, Ma XW, Liu NN, Tian NL, Gao XF, Xiao PX. Evaluation on the impact of spontaneous reperfusion on cardiac muscle of acute myocardial infarction by three-dimensional speckle tracking imaging. Eur Rev Med Pharmacol Sci 2017; 21: 5445-5450.
26) Bhatnagar P, Wickramasinghe K, Williams J, Rayner M, Townsend N. The epidemiology of cardiovascular disease in the UK 2014. Heart 2015; 101: 1182-1189.
27) Casas-Rojo E, Fernández-Golfin C, Moya-Mur JL, González-Gómez A, García-Martín A, Morán-Fernández L, Rodríguez-Muñoz D, Jiménez-Nacher JJ, Zamorano Gómez JL. Area strain from 3D speckle-tracking echocardiography as an independent predictor of early symptoms or ventricular dysfunction in asymptomatic severe mitral regurgitation with preserved ejection fraction. Int J Cardiovasc Imaging 2016; 32: 1189-1198.
28) Bhatt AS, Ambrosy AP, Velazquez EJ. Adverse Remodeling and reverse remodeling after myocardial infarction. Curr Cardiol Rep 2017; 19: 71.
29) Sari M, Kahveci G, Bayrak DF, Uslu A, Pala S. The other side of the coin in primary tricuspid valve disease: The incremental value of 3D echocardiography. Turk Kardiyol Dern Ars 2018; 46: 309-312.
30) Tian XF, Ji FJ, Zang HL, Cao H. Activation of the miR-34a/SIRT1/p53 signaling pathway contributes to the progress of liver fibrosis via inducing apoptosis in hepatocytes but not in HSCs. Plos One 2016; 11: e0158657.
31) Bordone L, Guarente L. Calorie restriction, SIRT1 and metabolism: understanding longevity. Nat Rev Mol Cell Biol 2005; 6: 298-305.
32) Yuan Y, Cruzat V F, Newshome P, Cheng J, Chen Y, Lu Y. Regulation of SIRT1 in aging: roles in mitochondrial function and biogenesis. Mech Ageing Dev 2016; 155: 10-21.
33) Simmons GE, Pruitt WM, Pruitt K. Diverse roles of SIRT1 in cancer biology and lipid metabolism. Int J Mol Sci 2015; 16: 950-965.
34) Takikawa A, Usui I, Fujisaka S, Ikutani M, Senda S, Hattori S, Tsuneyama K, Koshimizu Y, Inoue R, Tanaka-Hayashi A, Nakagawa T, Nagai Y, Takatsu K, Sasaoka T, Mori H, Tobe K. Deletion of SIRT1 in myeloid cells impairs glucose metabolism with enhancing inflammatory response to adipose tissue hypoxia. Diabetol Int 2015; 7: 59-68.
35) Meng X, Tan J, Li M, Song S, Miao Y, Zhang Q. Sirt1: role under the condition of ischemia/hypoxia. Cell Mol Neurobiol 2017; 37: 17-28.
36) Yamamoto T, Tamaki K, Shirakawa K, Ito K, Yan X, Katsumata Y, Anzai A, Matsuhashi T, Endo J, Inaba T, Tsubota K, Sano M, Fukuda K, Shinmura K. Cardiac Sirt1 mediates the cardioprotective effect of caloric restriction by suppressing local complement system activation after ischemia-reperfusion. Am J Physiol Heart Circ Physiol 2016; 310: H1003-H10014.
37) Gao P, Xu TT, Lu J, Li L, Xu J, Hao DL, Chen HZ, Liu DP. Overexpression of SIRT1 in vascular smooth muscle cells attenuates angiotensin II-induced vascular remodeling and hypertension in mice. J Mol Med (Berl) 2014; 92: 347-357.
38) Chen CJ, Yu W, Fu YC, Wang X, Li JL, Wang W. Resveratrol protects cardiomyocytes from hypoxia-induced apoptosis through the SIRT1–FoxO1 pathway. Biochem Biophys Res Commun 2009; 378: 389-393.
39) Hu YX, Cui H, Fan L, Pan XJ, Wu JH, Shi SZ, Cui SY, Wei ZM, Liu L. Resveratrol attenuates left ventricular remodeling in old rats with COPD induced by cigarette smoke exposure and LPS instillation. Can J Physiol Pharmacol 2013; 91: 1044-1054.
40) Zhang J, Wang QZ, Zhao SH, Ji X, Qiu J, Wang J, Zhou Y, Cai Q, Zhang J, Gao HQ. Astaxanthin attenuated pressure overload-induced cardiac dysfunction and myocardial fibrosis: Partially by activating SIRT1. Biochim Biophys Acta Gen Subj 2017; 1861: 1715-1728.
41) Sun XL, Bu PL, Liu JN, Wang X, Wu XN, Zhao LX. Expression of SIRT1 in right auricle tissues and the relationship with oxidative stress in patients with atrial fibrillation. Xi Bao Yu Fen Zi Mian Yi Xue Za Zhi 2012; 28: 972-974.
42) Guo Y, Zhang L, Li F, Hu CP, Zhang Z. Restoration of sirt1 function by pterostilbene attenuates hypoxia-reoxygenation injury in cardiomyocytes. Eur J Pharmacol 2016; 776: 26-33.
43) Li D, Wang X, Huang Q, Li S, Zhou Y, Li Z. Cardioprotection of CAPE-oNO2 against myocardial ischemia/reperfusion induced ROS generation via regulating the SIRT1/eNOS/NF-κB pathway in vivo and in vitro. Redox Biol 2018; 15: 62-73.
44) Zhou L, Wang SI, Moon YJ, Kim KM, Lee KB, Park BH, Jang KY, Kim JR. Overexpression of SIRT1 prevents hypoxia induced apoptosis in osteoblast cells. Mol Med Rep 2017; 16: 2969-2975.
45) D'Onofrio N, Servillo L, Balestrieri ML. SIRT1 and SIRT6 signaling pathways in cardiovascular disease protection. Antioxid Redox Signal 2018; 28: 711-732.
46) Qiu R, Wen L, Liu Y. MicroRNA-204 protects H9C2 cells against hypoxia/reoxygenation-induced injury through regulating SIRT1-mediated autophagy. Biomed Pharmacother 2018; 100: 15-19.
47) Aşci H, Saygin M, Đükriye Yeşilot, Topsakal S, Özlem Özmen Cankara, Nihan F, Savran M. Protective effects of aspirin and vitamin C against corn syrup consumption-induced cardiac damage through sirtuin-1 and HIF-1a pathway. Anatol J Cardiol 2016; 16: 648-654.
48) Deng M, Wang D, He S, Xu R, Xie Y. SIRT1 confers protection against ischemia/reperfusion injury in cardiomyocytes via regulation of uncoupling protein 2 expression. Mol Med Rep 2017; 16: 7098-7104.